

TITLE OF SYMPOSIUM: 31st National Symposium on Fatigue and Fracture Mechanics

AUTHORS' NAMES:

Sreeramesh Kalluri¹, Michael A. McGaw², and Gary R. Halford³

TITLE OF PAPER: Fatigue Life Estimation under Cumulative Cyclic Loading Conditions

(Paper ID # 8136)

AUTHORS' AFFILIATIONS:

¹Senior Research Engineer, Ohio Aerospace Institute, Brookpark, Ohio.

²President, McGaw Technology, Inc., Lakewood, Ohio.

³Senior Scientific Technologist, Research and Technology Directorate, NASA Glenn Research Center, Cleveland, Ohio.

ABSTRACT: The cumulative fatigue behavior of a cobalt-base superalloy, Haynes 188 was investigated at 760°C in air. Initially strain-controlled tests were conducted on solid cylindrical gauge section specimens of Haynes 188 under fully-reversed, tensile and compressive mean strain-controlled fatigue tests. Fatigue data from these tests were used to establish the baseline fatigue behavior of the alloy with 1) a total strain range type fatigue life relation and 2) the Smith-Watson-Topper (SWT) parameter. Subsequently, two load-level multi-block fatigue tests were conducted on similar specimens of Haynes 188 at the same temperature. Fatigue lives of the multi-block tests were estimated with 1) the Linear Damage Rule (LDR) and 2) the nonlinear Damage Curve Approach (DCA) both with and without the consideration of mean stresses generated during the cumulative fatigue tests. Fatigue life predictions by the nonlinear DCA were much closer to the experimentally observed lives than those obtained by the LDR. In the presence of mean stresses, the SWT parameter estimated the fatigue lives more accurately under tensile conditions than under compressive conditions.

KEYWORDS: cumulative fatigue, cyclic hardening, damage curve approach, life prediction, linear damage rule, mean strain, mean stress

Nomenclature

- b, c Exponents of elastic and inelastic strain range-life relations
- n Number of applied cycles at a load level in a cumulative fatigue test
- B, C Coefficients of elastic and inelastic strain range-life relations
- D Damage
- E Modulus of elasticity
- N Number of cycles in a single load-level test or blocks in a two load-level test

R	Ratio of minimum value to maximum value in a cycle
ε	Engineering strain
Δ	Denotes range of a variable
σ	stress

Subscripts

1	First load-level in a two load-level cumulative fatigue test
2	Second load-level in a two load-level cumulative fatigue test
B	Blocks
f	Failure
el	Elastic
in	Inelastic
k	Number of blocks at failure in a multi-block fatigue test
m	Mean
t	Total

Introduction

The determination of fatigue life under cyclically interactive loading conditions is necessary to assess the durability of many engineering components routinely used in terrestrial and aerospace applications. Limitations on the durability of components subjected to cumulative fatigue loading can severely restrict their usage both due to cost and safety considerations. Fatigue life prediction models capable of estimating accurately the durability of engineering components under cumulative loading conditions (involving two or more cyclic loads) are required to avoid unnecessary over design as well as under design that can potentially lead to catastrophic failures.

Many cumulative fatigue investigations conducted in the past involve mainly two load-level single-block tests [1-12]. In such tests, mean stresses and strains are typically avoided at both load levels by careful design of the experiments. The fatigue lives obtained from the single-block (i.e., "one step") tests are commonly utilized to document the ordering effects (high/low or low/high) in cumulative damage studies. By comparison cumulative fatigue studies under two load-level, multi-block loading conditions that include mean stresses at one or both load levels are fewer in number [13-16]. Fatigue life predictions under cumulative fatigue loading conditions that include mean stresses are difficult tasks because they must consider 1) the influence of mean stress (either tensile or compressive) on the material's fatigue behavior and 2) the accumulation of fatigue damage from different load levels and the associated damage interaction.

The objective of the present investigation was to estimate the cumulative fatigue life of a cobalt-base superalloy, Haynes 188, in the presence of mean stresses (either tensile or compressive) under two load-level, multi-block loading conditions. Haynes 188 has applications as a combustor liner material in aeronautical propulsion system components and as a cryogenic oxygen carrying tube material in the main injector of the reusable space shuttle main engine. The tensile ductility of this material exhibits a minimum around 760°C [17]. Since low-cycle fatigue life of a material is predominantly governed by ductility, this temperature was selected for the present investigation to obtain a lower bound on life over the temperature range of application. Two load-level, single block tests were previously conducted at 760°C by Bizon et al. on Haynes 188 [7]. They reported significant cumulative fatigue damage interaction in the high/low type of two load-level single-block tests. In the present study, initially strain-controlled fatigue tests were conducted at three different mean strain conditions (fully-reversed, tensile, and

compressive) at 760°C on cylindrical specimens machined from Haynes 188, a wrought cobalt-base superalloy. The fatigue data generated from these tests were used to characterize the baseline strain-controlled fatigue behavior of Haynes 188 and the influence of mean strain on fatigue life. Subsequently, two load-level multi-block cyclic loading experiments were conducted to evaluate the influences of both tensile and compressive mean stresses and strains under cumulative fatigue conditions. The fatigue lives of the specimens tested in cumulative fatigue were estimated by the Linear Damage Rule (LDR) [1, 18, 19] and the nonlinear Damage Curve Approach (DCA) [4, 8] both with and without the consideration of the tensile and compressive mean stresses generated during the multi-block tests. The results from the experimental program on Haynes 188 superalloy and a comparison of the predictive capabilities of the LDR and DCA methods are discussed.

Material and Specimens

Wrought cobalt-base superalloy, Haynes 188, was supplied by a commercial vendor in the form of bars with a nominal diameter of 19.1 mm. The bars were hot-rolled, centerless ground, and solution-annealed by the manufacturer (heat number: 1880-8-1742). The chemical composition of the superalloy in weight percent is as follows: <0.002 S, 0.002 B, 0.012 P, 0.1 C, 0.4 Si, 0.034 La, 0.75 Mn, 1.24 Fe, 13.95 W, 21.84 Cr, 22.43 Ni, with the balance being cobalt. Solid, cylindrical fatigue specimens with a nominal gauge section diameter of 6.4 mm were machined from the bars. The final machining step involved mechanically polishing the gauge section of every specimen along the longitudinal direction.

Experimental Details

All the tests were conducted in a servohydraulic rig equipped with hydro-collet grips. The specimens were heated to the test temperature of 760°C in air within a three-coil induction

heating fixture. A commercially available, water-cooled extensometer with a gauge length of 12.7 mm was used to measure displacement within the gauge section of each specimen. The temperature of the specimen in the gauge section was monitored with a noncontacting optical temperature measurement system. Temperature control was accomplished by chromel-alumel (Type K) thermocouples spot-welded on the shoulders of the specimen. Test control and data acquisition for baseline mean strain-controlled tests and the two load-level multi-block tests were performed with control-tree based software [20]. The software version used in this study [21] was executed on a personal computer that contained the necessary analog to digital and digital to analog converters and was interfaced with the servocontroller. In all of the fatigue tests, a cyclic frequency of 0.1 Hz was used and failure was defined either as a 50% drop in tensile load from the maximum value or separation of the specimen into two pieces, whichever occurred first.

Results

Baseline Tests

Baseline strain-controlled fatigue tests were conducted on Haynes 188 specimens at 760°C under fully-reversed ($R_\epsilon = -1$), tensile ($R_\epsilon = 0$), and compressive ($R_\epsilon = -\infty$) mean strain conditions. Baseline fatigue data obtained from the near half-life hysteresis loops are listed in Table 1. The average elastic modulus (171 GPa) of Haynes 188 at 760°C was used to compute the elastic strain range from the observed stress range for each test. The inelastic strain range was then obtained for each test by subtracting the elastic strain range from the total strain range. A total strain range versus fatigue life relation (Eq. 1) was used to characterize the strain-controlled fatigue data:

$$\Delta\varepsilon_t = B(N_f)^b + C(N_f)^c \quad (\text{Eq. 1})$$

Constants and exponents in the life relation were obtained by performing least square regression fits between logarithms of elastic strain range and fatigue life as well as inelastic strain range and fatigue life for fully-reversed ($R_\varepsilon = -1$), tensile ($R_\varepsilon = 0$), and compressive ($R_\varepsilon = -\infty$) mean strain conditions (Table 2). In computing the constants shown in Table 2, any runout data shown in Table 1 were omitted. The elastic, inelastic, and total strain range life relations for the fully-reversed condition are shown in Fig. 1. Arrows in this figure identify runout data. Fatigue data from tensile ($R_\varepsilon = 0$) and compressive ($R_\varepsilon = -\infty$) mean strain-controlled tests are plotted together with the total strain range life relationship from the fully-reversed ($R_\varepsilon = -1$) tests in Fig. 2.

Fatigue data from tensile and compressive mean strain-controlled tests agree closely with the life relationship obtained from the fully-reversed tests. The evolution of stress ranges and mean stresses for two selected strain ranges ($\Delta\varepsilon = 0.02$ and 0.005) are shown for the baseline tests in Fig. 3. Haynes 188 exhibited cyclic hardening at both strain ranges at 760°C (Fig. 3(a)). Moreover, at the strain range of 0.005 , mean strain (tensile or compressive) did not significantly influence the cyclic hardening behavior of the superalloy. Under fully-reversed conditions, Haynes 188 developed small magnitudes of compressive mean stresses which prevailed through the duration of the fatigue tests (Fig. 3(b) and Table 1). In the specimens tested under tensile and compressive mean strain conditions, during the initial cycles tensile and compressive mean stresses, respectively, were observed (Fig. 3(b)). However, these mean stresses relaxed over a few cycles and only small magnitude compressive mean stresses (similar to those observed in fully-reversed tests) prevailed near and beyond the half-life durations in these tests (Table 1). Relaxation of the mean stresses in the mean strain-controlled tests is the primary reason for the

close agreement observed earlier (Fig. 2) between the fatigue data generated in these tests and the fatigue life relationship obtained from the fully-reversed fatigue tests. Since no significant differences in fatigue life were observed in fatigue lives of fully-reversed and mean strain-controlled fatigue tests, data from all these tests were combined and a total strain range life relationship (Eq. 1) was calculated. This life relationship (constants and exponents listed in Table 2) was subsequently used to estimate fatigue lives in the cumulative fatigue damage tests without mean stress consideration.

In order to estimate fatigue life in the presence of mean stresses a model that accounts for their influence on fatigue life is necessary⁴. The Smith-Watson-Topper (SWT) parameter [22], (Eq. 2a), was selected to estimate fatigue life of Haynes 188 under mean stress conditions. This parameter was previously used successfully to estimate the fatigue life of another superalloy, Inconel 718, under mean stress conditions [11].

$$\text{SWT} = \sigma_{\max} \left(\frac{\Delta \varepsilon_t}{2} \right) E = A_1 (N_f)^{a_1} + A_2 (N_f)^{a_2} \quad (\text{Eq. 2a})$$

Fatigue data from the fully-reversed and tensile and compressive mean strain-controlled tests were combined to obtain the SWT fatigue life parameter (Eq. 2b) for Haynes 188 at 760°C (Fig. 4).

$$\sigma_{\max} \left(\frac{\Delta \varepsilon_t}{2} \right) E = 6.74 \times 10^5 (N_f)^{-0.165} + 5.86 \times 10^7 (N_f)^{-0.815} \quad (\text{Eq. 2b})$$

This parameter was subsequently used to estimate fatigue lives in the cumulative fatigue damage tests with mean stress consideration.

⁴ The fatigue data generated on Haynes 188 under tensile and compressive mean strain-controlled conditions could not be used for this purpose because of the observed mean stress relaxation in these tests.

Cumulative Fatigue Tests

Two types of block loading patterns (Fig. 5) were designed to perform the two load-level multi-block fatigue tests on Haynes 188 at 760°C. In both of these block loading patterns, each block consisted of one major cycle with a strain range of $\Delta\epsilon = 0.02$ and 50 minor cycles with a lower strain range, $\Delta\epsilon = 0.005$. The major cycle was fully-reversed in both of the block loading patterns (B1 and B2). In the case of block loading B1 the minor cycles were applied with $R_\epsilon = 0.5$ (Fig. 5(a)), whereas in block loading B2 the minor cycles were applied with $R_\epsilon = 2$ (Fig. 5(b)). Duplicate fatigue tests were conducted with block loading patterns B1 and B2. Hysteresis loops generated during the multi-block fatigue tests are shown in Fig. 6. Block loading B1 lead to a tensile mean stress in the minor cycles ((Fig. 6(a)), whereas a compressive mean stress was observed in the minor cycles during block loading B2 (Fig. 6(b)). In both types of block loading patterns, the mean stresses relaxed slightly over the 50 minor cycles within a block of loading (Fig. 7). However, even during the 50th minor cycle, the magnitudes of the mean stresses were significantly large in both cases. Cumulative fatigue data obtained from the near half-life blocks in the two load-level, multi-block tests are listed in Table 3. Hysteresis loops corresponding to the major cycle and the 25th minor cycle were used to obtain the data shown in Table 3. Even though the cumulative fatigue data are limited, on the average block loading B2, which lead to compressive mean stresses in the minor cycles, exhibited slightly higher fatigue lives than block loading B1.

Fatigue Life Estimation

Fatigue lives in the cumulative fatigue tests were estimated with LDR (Eq. 3) and nonlinear DCA (Eq. 4) both with and without the consideration of the tensile and compressive mean stresses generated during the multi-block cyclic loading conditions.

$$D(n_1, N_1) = \left(\frac{n_1}{N_1} \right) \quad (\text{Eq. 3})$$

$$D(n_2, N_2) = \left(\frac{n_2}{N_2} \right)$$

In LDR [1,18,19], the damage from the first and second load levels is defined in terms of the life fractions at each of those loads. In the case of nonlinear DCA [4,8] damage at the first load level is defined as the life fraction, however, at the second load level it is a nonlinear function of the life fraction and is dependent on the ratio of the baseline fatigue lives at the two load levels.

$$D(n_1, N_1) = \left(\frac{n_1}{N_1} \right) \quad (\text{Eq. 4})$$

$$D(n_2, N_2) = \left(\frac{n_2}{N_2} \right) \left(\frac{N_2}{N_1} \right)^{0.4}$$

For both models $D=0$ for the undamaged (or untested) state and $D=1$ at final failure. For the multi-block tests with two load levels, both models predict failure when the following condition is satisfied.

$$\sum_{i=1}^k [D_i(n_1, N_1) + D_i(n_2, N_2)] = 1 \quad (\text{Eq. 5})$$

where, subscript $i=1$, k denotes the block number.

The accumulation of fatigue damage in the case of LDR is linear at all life levels and is obtained by an algebraic sum of the life fractions at the two load levels within a block and then by the addition of damage associated with each block of loading. Damage accumulation in the DCA is more complicated and is illustrated in Fig. 8. For every block of loading with the DCA, fatigue damage sustained by the material at each load level must be tracked by the damage curve associated with that load level. For example, during the first block of loading, damage due to the

first load level is indicated by point A in Fig. 8. In order to evaluate the damage from the second load level during the first block of loading, initially point A must be translated along a horizontal line to point B, which is on the damage curve (obtained by using Eq. 4) associated with the second load level. The damage from the second load level is represented by BC. At this stage, to assess the damage from the first load level during the second block of loading, point C must again be translated horizontally to point D on the damage curve for the first load level. The damage from the two load levels in each succeeding block must be accumulated in a repetitive manner until the criterion for failure (Eq. 5) is satisfied. The entire damage calculation process for the two load-level multi-block tests was performed with two computer programs for the LDR and DCA methods.

Fatigue lives of the two load-level, multi-block tests estimated by LDR and DCA without mean stress consideration are shown in Fig. 9(a). The baseline fatigue lives (N_1 and N_2) for this analysis were obtained with the total strain range life relation (Eq. 1 and Table 2) by combining all the strain-controlled fatigue data ($R_e = -\infty, -1, \& 0$). In general, for both types of block loading patterns (B1 and B2), when mean stresses were not considered, the fatigue life predictions by the LDR were highly nonconservative compared to the life estimations by the DCA. Fatigue life estimations by LDR and DCA for the cumulative fatigue tests with mean stress consideration are shown in Fig. 9(b). The SWT parameter (Eq. 2b) was used to obtain N_1 and N_2 values for the analysis. As in the previous case, the predicted lives by the LDR were higher than those estimated by the DCA for block loading patterns B1 and B2. Both LDR and DCA were able to predict the fatigue lives under block loading B1, which resulted in a tensile mean stress at the second load level, to within approximately 25 blocks of the experimentally observed lives. However, for block loading B2, which resulted in compressive mean stress at

the second load level, predictions by both LDR and DCA were worse than when mean stresses were ignored.

Discussion

In this study, no significant differences were observed among the fatigue lives of the baseline fatigue tests conducted under fully-reversed ($R_\epsilon = -1$), tensile ($R_\epsilon = 0$), and compressive ($R_\epsilon = -\infty$) mean strain conditions (Figs. 1 & 2 and Table 2). This is mainly due to the relaxation of the mean stresses in the tensile ($R_\epsilon = 0$), and compressive ($R_\epsilon = -\infty$) mean strain-controlled tests to the levels observed in the fully-reversed strain-controlled tests (Fig. 3 and Table 1). The extent of mean stress relaxation in the mean strain-controlled tests depends upon the ductility of the material, test temperature, and strain range. For Haynes 188 at 760°C, the test conditions in this study facilitated the relaxation of the mean stresses observed during the initial cycles. However, for high strength materials with low ductility and at moderate temperatures such a mean stress relaxation may not occur in mean strain-controlled tests. Therefore, the influence of mean strain and the associated manifestation of mean stress must be carefully ascertained for each material and test condition.

Under cumulative fatigue loading conditions, regardless of the method used for damage accumulation (LDR or nonlinear DCA), the SWT parameter was able to improve the fatigue life predictions for tensile mean stress conditions (Fig. 9, Block Loading: B1). However, for compressive mean stress conditions (Fig. 9, Block Loading: B2) predictions by the same parameter were worse (higher) than when no mean stress influence was considered. These results indicated that for Haynes 188 at 760°C the SWT parameter accurately represented the detrimental influence of tensile mean stress on the fatigue life. However, this parameter overestimated the beneficial effect of compressive mean stress on the fatigue life of Haynes 188.

Note that the SWT parameter (Eq. 2a) can not be used to estimate the fatigue life under complex cumulative fatigue loading conditions that lead to a hysteresis loop with a compressive maximum stress. In such cases, either the effect of mean stress on fatigue life can be ignored or another method should be employed to determine the influence of compressive mean stress on fatigue life.

For the two load-level, multi-block tests (whether the influence of mean stress on fatigue life was considered or ignored) predicted fatigue lives by the nonlinear DCA were much closer to the experimentally observed fatigue lives than those by the LDR. This observation implies that fatigue damage tends to accumulate in the multi-block tests in a nonlinear fashion. The methodology used in this study for cumulative fatigue life estimation with DCA can be extended to a multi-block loading with multiple load levels. Under these circumstances, after selecting a load level for the reference life, the damage curves for all the load levels need to be determined using equations similar to Eqs. 4 and 5. Fatigue life calculations can be performed by carefully keeping track of each damage curve and switching among the curves, while computing the damage from each load level within a block of loading, and by adding the damage from all the blocks until the failure criterion is satisfied.

Summary

The cumulative fatigue behavior of a cobalt-base superalloy, Haynes 188 at 760°C was investigated by conducting baseline fully-reversed, tensile, and compressive mean strain-controlled tests and two load-level multi-block fatigue tests. No significant differences were observed among the fatigue lives of the fully-reversed, tensile, and compressive mean strain-controlled fatigue tests mainly due to the relaxation of mean stresses in the tensile and compressive mean strain-controlled tests. The fatigue behavior of the baseline tests was

adequately characterized by both 1) the total strain range versus fatigue life relation and 2) the Smith-Watson-Topper parameter. Fatigue lives of the two load-level, multi-block tests were estimated by the Linear Damage Rule and the nonlinear Damage Curve Approach both with and without the consideration of the influence of mean stress on the fatigue life. In general, predictions by the method of nonlinear damage curve were much closer to the experimentally observed fatigue lives. In the presence of tensile mean stresses, the Smith-Watson-Topper parameter improved cumulative fatigue life predictions. However, under compressive mean stress conditions this parameter overestimated the beneficial effect on fatigue life.

Acknowledgment

The assistance provided by Mr. Christopher S. Burke (Dynacs Engineering Company, Inc.) for performing all the tests in the High Temperature Fatigue and Structures Laboratory is gratefully acknowledged.

References

- [1] Miner, M. A., "Cumulative Damage in Fatigue," *Journal of Applied Mechanics*, Vol. 12, No. 3, September 1945, (*Transactions of the American Society of Mechanical Engineers*, Vol. 67, 1945), pp. A159-A164.
- [2] Manson, S. S., Nachtigall, A. J., Ensign, C. R., and Freche, J. C., "Further Investigation of a Relation for Cumulative Fatigue Damage in Bending," *Journal of Engineering for Industry*, Vol. 87, 1965, pp. 25-35.
- [3] Wood, W. A. and Reimann, W. H., "Observations on Fatigue Damage Produced by Combinations of Amplitudes in Copper and Brass," *Journal of the Institute of Metals*, Vol. 94, 1966, pp. 66-70.

- [4] Manson, S. S. and Halford, G. R., "Practical Implementation of the Double Linear Damage Rule and Damage Curve Approach for Treating Cumulative Fatigue Damage," *International Journal of Fracture*, Vol. 17, No. 2, 1981, pp. 169-192.
- [5] Miller, K. J. and Ibrahim, M. F. E., "Damage Accumulation During Initiation and Short Crack Growth Regimes," *Fatigue of Engineering Materials and Structures*, Vol. 4, No. 3, 1981, pp. 263-277.
- [6] Bui-Quoc, T., "Cumulative Damage with Interaction Effect due to Fatigue Under Torsion Loading," *Experimental Mechanics*, 1982, pp. 180-187.
- [7] Bizon, P. T., Thoma, D. J., and Halford, G. R., "Interaction of High Cycle and Low Cycle Fatigue of Haynes 188 at 1400°F," *Structural Integrity and Durability of Reusable Space Propulsion Systems*, NASA CP-2381, 1985, pp. 139-145.
- [8] Manson, S. S., and Halford, G. R., "Re-examination of Cumulative Fatigue Damage Analysis -- An Engineering Perspective", *Engineering Fracture Mechanics*, Vol. 25, Nos. 5/6, 1986, pp. 539-571.
- [9] Golos, K. and Ellyin, F., "Generalization of Cumulative Damage Criterion to Multilevel Cyclic Loading," *Theoretical and Applied Fracture Mechanics*, Vol. 7, 1987, pp. 169-176.
- [10] Chaboche, J. L. and Lesne, P. M., "A Non-Linear Continuous Fatigue Damage Model," *Fatigue and Fracture of Engineering Materials and Structures*, Vol. 11, No. 1, 1988, pp. 1-17.
- [11] Kalluri, S., Halford, G. R., and McGaw, M. A., "Prestraining and its Influence on Subsequent Fatigue Life," *Advances in Fatigue Lifetime Predictive Techniques: 3rd*

- Volume*, ASTM STP 1292, M. R. Mitchell and R. W. Landgraf, Eds., American Society for Testing and Materials, 1996, pp. 328-341.
- [12] Kalluri, S., and Bonacuse, P. J., "Cumulative Axial and Torsional Fatigue: An Investigation of Load-Type Sequencing Effects," Paper Presented at the ASTM Symposium on Multiaxial Fatigue and Deformation: Testing and Prediction, held during May 19-20, 1999 in Seattle, Washington.
- [13] Dowling, N. E., "Fatigue Failure Predictions for Complicated Stress-Strain Histories," *Journal of Materials*, JMLSA, Vol. 7, No. 1, March 1972, pp. 71-87.
- [14] Walcher, J., Gray, D., and Manson, S. S., "Aspects of Cumulative Fatigue Damage Analysis of Cold End Structures," 79-1190, AIAA/SAE/ASME 15th Joint Propulsion Conference, June 18-20, 1979, Las Vegas, Nevada, pp. 1-13.
- [15] Vasek, A., and Polak, J., "Low Cycle Fatigue Damage Accumulation in Armco-Iron," *Fatigue and Fracture of Engineering Materials and Structures*, Vol. 14, No. 2/3, 1991, pp. 193-204.
- [16] McGaw, M. A., Kalluri, S., Moore, D., and Heine, J., "The Cumulative Fatigue Damage Behavior of Mar-M 247 in Air and High Pressure Hydrogen," *Advances in Fatigue Lifetime Predictive Techniques: Second Volume*, ASTM STP 1211, M. R. Mitchell and R. W. Landgraf, Eds., American Society for Testing and Materials, 1993, pp. 117-131.
- [17] Nickel Base Alloys, International Nickel Company, New York, 1977.
- [18] Palmgren, A., "Die Lebensdauer von Kugellagern," *Zeitschrift des Vereinesdeutscher Ingenieure*, Vol. 68, No. 14, April 1924, pp. 339-341 (The Service Life of Ball Bearings, NASA Technical Translation of German Text, NASA TT 1-13460, 1971).

- [19] Langer, B. F., "Fatigue Failure from Stress Cycles of Varying Amplitude," *Journal of Applied Mechanics*, Vol. 4, No. 3, September 1937, (*Transactions of the American Society of Mechanical Engineers*, Vol. 59, 1937), pp. A160-A162.
- [20] McGaw, M.A. and Bonacuse, P.J., "Automation Software for a Materials Testing Laboratory," *Applications of Automation Technology to Fatigue and Fracture Testing*, ASTM STP 1092, A. A. Braun, N. E. Ashbaugh, and F. M. Smith, Eds., American Society for Testing and Materials, Philadelphia, 1990, pp. 211-231.
- [21] McGaw, M.A., "Materials Testing Software", LEW-16160, COSMIC, Athens, GA, 1995.
- [22] Smith, K. N., Watson, P., and Topper, T. H., "A Stress-Strain Function for the Fatigue of Metals," *Journal of Materials*, JMSLA, Vol. 5, No. 4, 1970, pp. 767-778.

Figure Captions

Fig. 1 -- Fatigue Life Relationships for Haynes 188 at 760°C, Fully Reversed ($R_\epsilon = -1$)

Fig. 2 -- Tensile ($R_\epsilon = 0$) and Compressive ($R_\epsilon = -\infty$) Mean Strain-Controlled Fatigue Data and Fully-Reversed ($R_\epsilon = -1$) Fatigue Life Relationship for Haynes 188 at 760°C

Fig. 3 -- Cyclic Stress Evolution in Strain-Controlled Baseline Fatigue Tests

a) Stress Ranges

b) Mean Stresses

Fig. 4 -- Smith-Watson-Topper Fatigue Life Relation for Strain-Controlled Fatigue Data ($R_\epsilon = -\infty, -1, \text{ and } 0$) of Haynes 188 at 760°C

Fig. 5 -- Schematics of Block Loading Patterns in Cumulative Fatigue Tests

a) Block Loading, B1

b) Block Loading, B2

Fig. 6 -- Hysteresis Loops in Cumulative Fatigue Tests

a) Block Loading, B1

b) Block Loading, B2

Fig. 7 -- Evolution of Mean Stresses in Cumulative Fatigue Tests

Fig. 8 -- Schematic of Damage Estimation in Two Load-Level Multi-Block Fatigue Tests with Nonlinear Damage Curve Approach

Fig. 9 -- Life Prediction of Cumulative Fatigue Tests: Haynes 188 at 760° C

a) Without Mean Stress Consideration

b) With Mean Stress Consideration

TABLE 1 – Strain-Controlled Fatigue Data of Haynes 188 at 760°C

Specimen Number	R_e	$\Delta\varepsilon_t$	$\Delta\sigma$ (MPa)	σ_m (MPa)	$\Delta\varepsilon_{cl}$	$\Delta\varepsilon_{in}$	N_f (Cycles)
HB29	-1	0.01980	1 077	-9	0.00630	0.01350	300
HB28	-1	0.01386	979	-8	0.00573	0.00813	584
HB22	-1	0.00990	852	-3	0.00498	0.00492	1 062
HB23	-1	0.00792	848	-4	0.00496	0.00296	2 043
HB26	-1	0.00692	794	-4	0.00464	0.00228	2 467
HB24	-1	0.00594	808	-3	0.00473	0.00121	6 364
HB25	-1	0.00494	710	-2	0.00415	0.00079	24 364
HB30	-1	0.00460	697	-3	0.00408	0.00052	42 752
HB27 ^a	-1	0.00396	674	-1	0.00394	0.00002	105 015
HB34	0	0.01385	1 006	-8	0.00588	0.00797	674
HB38	0	0.00990	909	-4	0.00532	0.00458	1 379
HB36	0	0.00792	846	-6	0.00495	0.00297	2 096
HB37	0	0.00596	780	-4	0.00456	0.00140	5 250
HB54	0	0.00495	793	-3	0.00464	0.00031	25 426
HB35	0	0.00453	734	-10	0.00429	0.00024	57 663
HB39	$-\infty$	0.01385	983	-4	0.00575	0.00810	648
HB42	$-\infty$	0.00991	872	-4	0.00510	0.00481	1 192
HB43	$-\infty$	0.00792	839	-4	0.00491	0.00301	2 282
HB44	$-\infty$	0.00611	781	-4	0.00457	0.00154	4 028
HB56	$-\infty$	0.00513	790	-6	0.00462	0.00051	28 465

^aTest was a runout

TABLE 2 – Constants for Total Strain Range - Fatigue Life Relationships

R_ϵ	b	c	B	C
-1	-0.0897	-0.660	0.0100	0.500
0	-0.0735	-0.833	0.00918	1.80
$-\infty$	-0.0796	-0.746	0.00938	0.940
$-\infty, -1, \& 0$	-0.0835	-0.751	0.00972	0.980

TABLE 3 - Cumulative Fatigue Data of Haynes 188 at 760°C

Specimen Number	Block Loading	Major Cycle				Minor Cycle				N_B (Blocks)
		R_ϵ	$\Delta\epsilon_t$	$\Delta\sigma$ (MPa)	σ_m (MPa)	R_ϵ	$\Delta\epsilon_t$	$\Delta\sigma$ (MPa)	σ_m (MPa)	
HB49	B1	-1	0.01980	1 130	-14	0.5	0.00493	791	106	71
HB45	B1	-1	0.01978	1 007	-12	0.5	0.00492	753	73	80
HB57	B2	-1	0.01980	1 151	-6	2.0	0.00493	833	-116	76
HB53	B2	-1	0.01978	1 245	-4	2.0	0.00493	851	-145	138

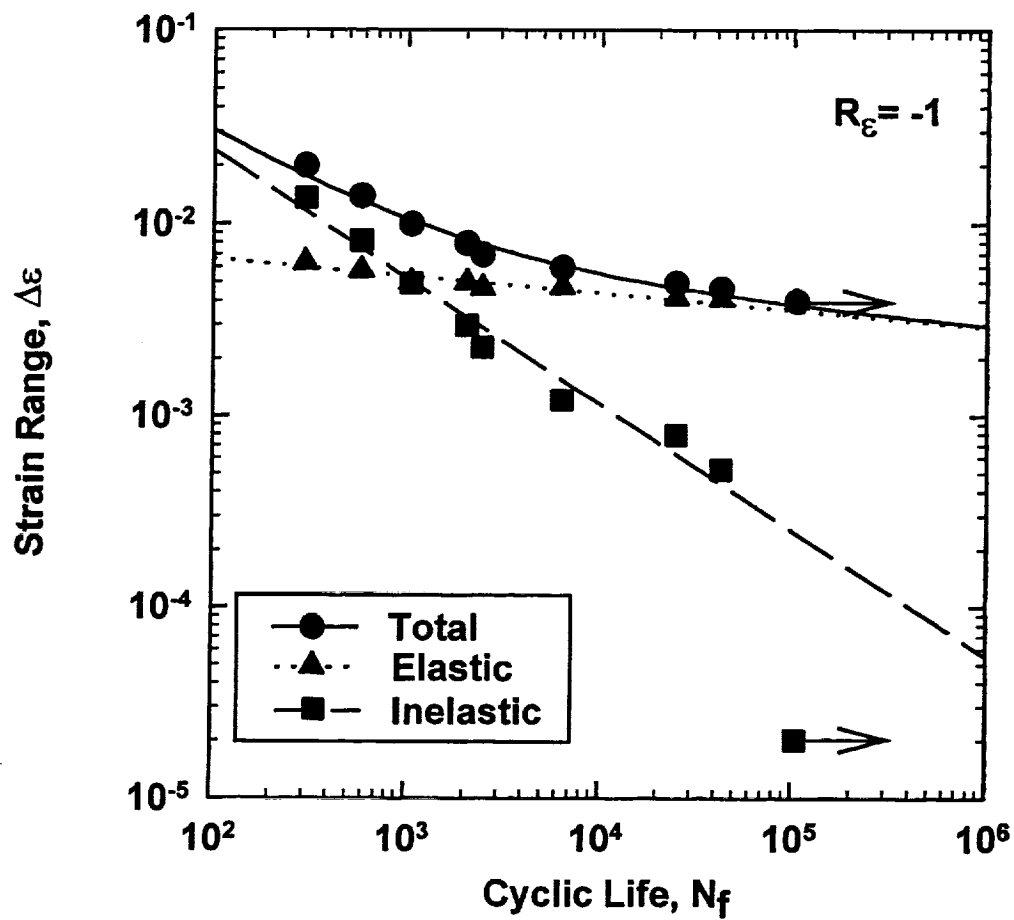


Fig. 1 -- Fatigue Life Relationships for Haynes 188 at 760°C, Fully Reversed ($R_\epsilon = -1$)

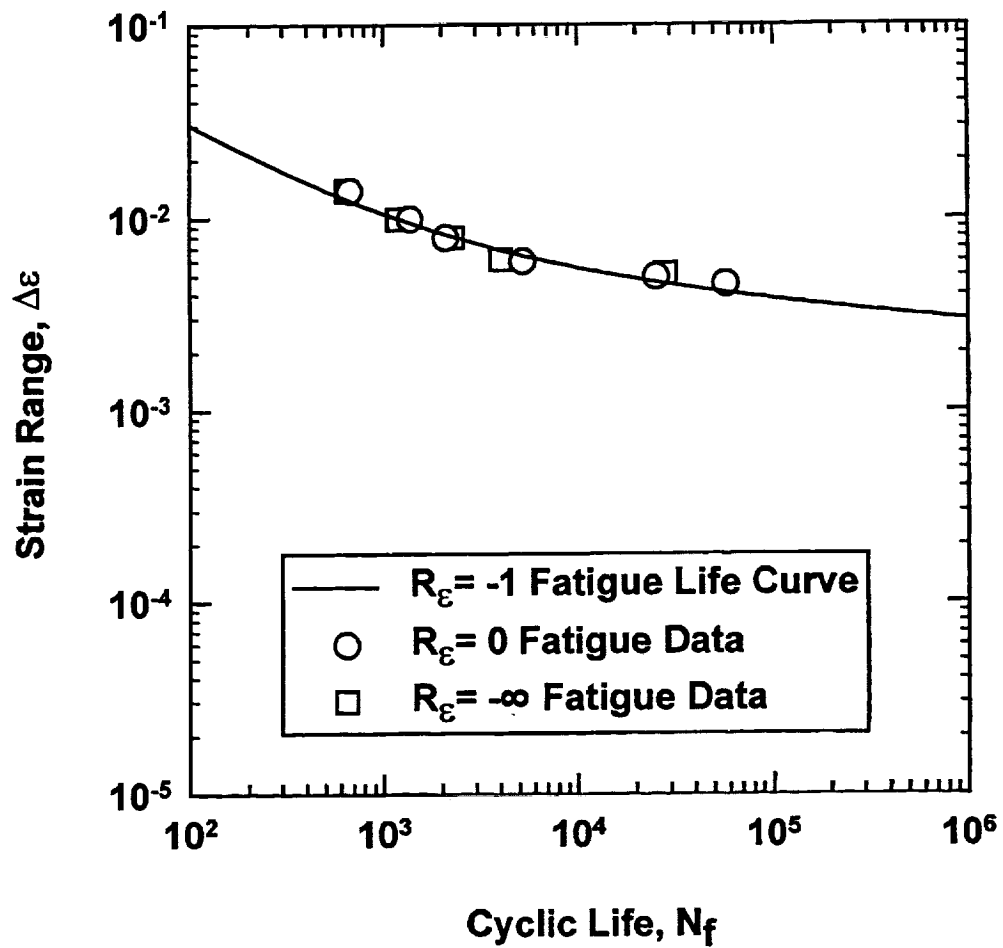
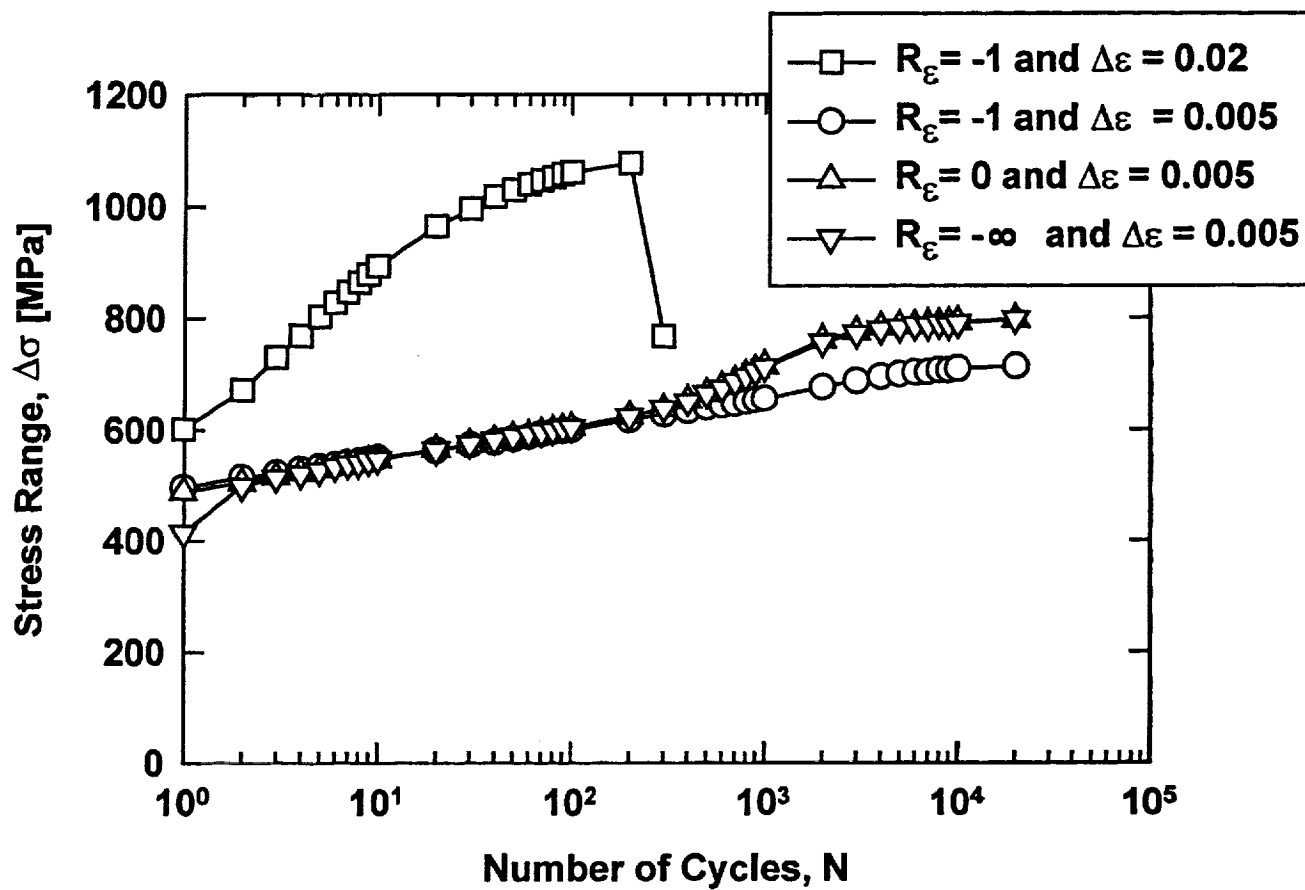
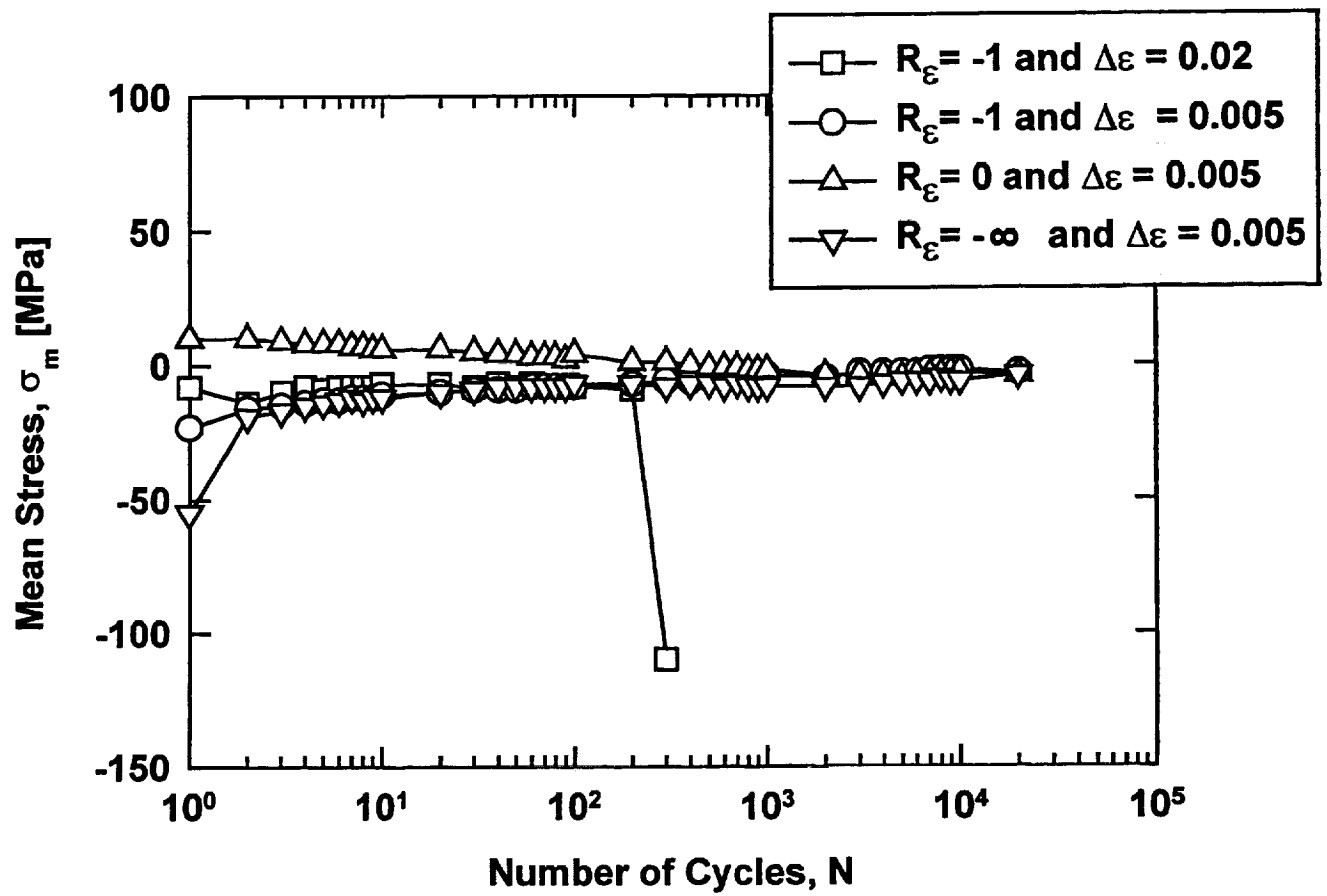


Fig. 2 -- Tensile ($R_\varepsilon = 0$) and Compressive ($R_\varepsilon = -\infty$) Mean Strain-Controlled Fatigue Data and Fully-Reversed ($R_\varepsilon = -1$) Fatigue Life Relationship for Haynes 188 at 760°C



a) Stress Ranges

Fig. 3 -- Cyclic Stress Evolution in Strain-Controlled Baseline Fatigue Tests



b) Mean Stresses

Fig. 3 -- Cyclic Stress Evolution in Strain-Controlled Baseline Fatigue Tests

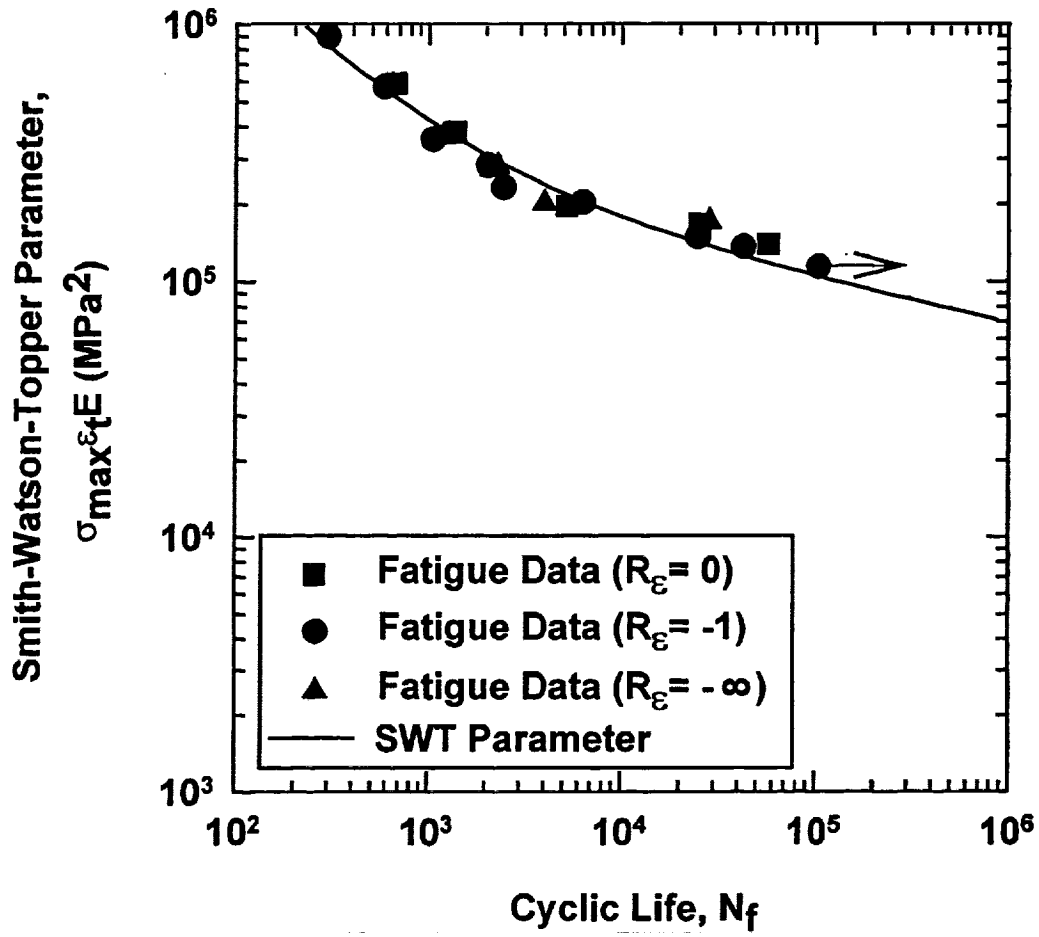
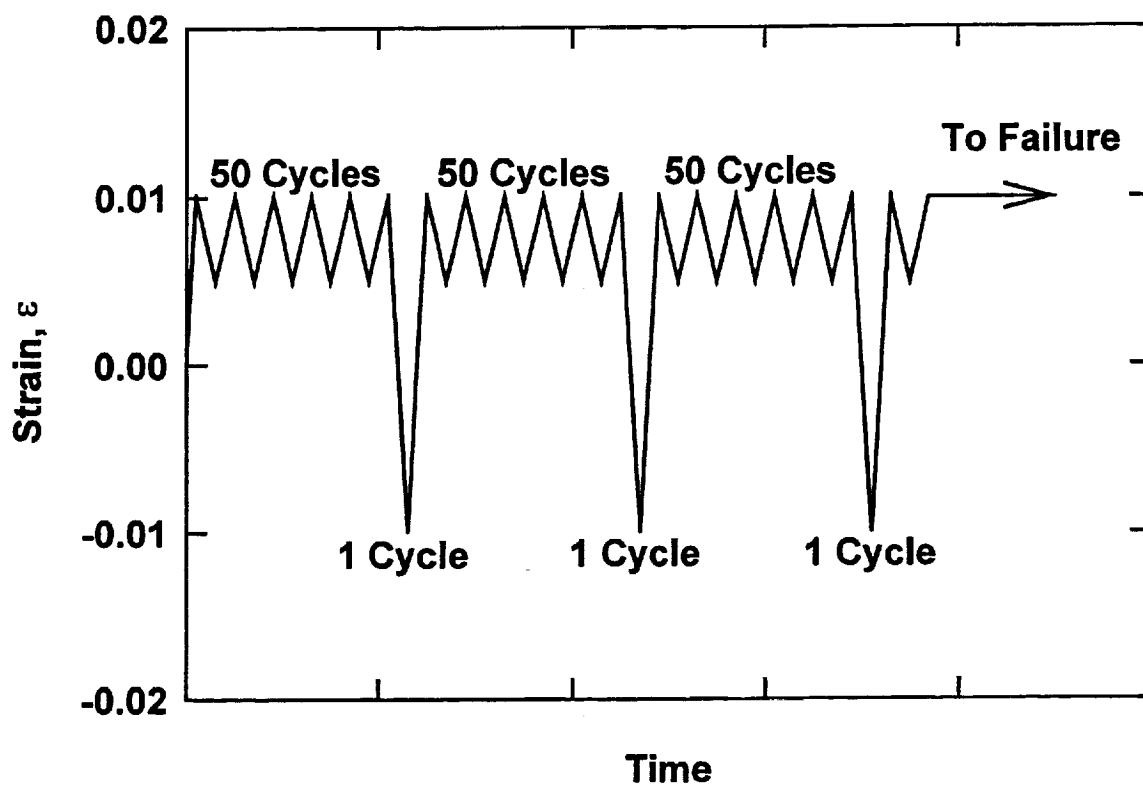


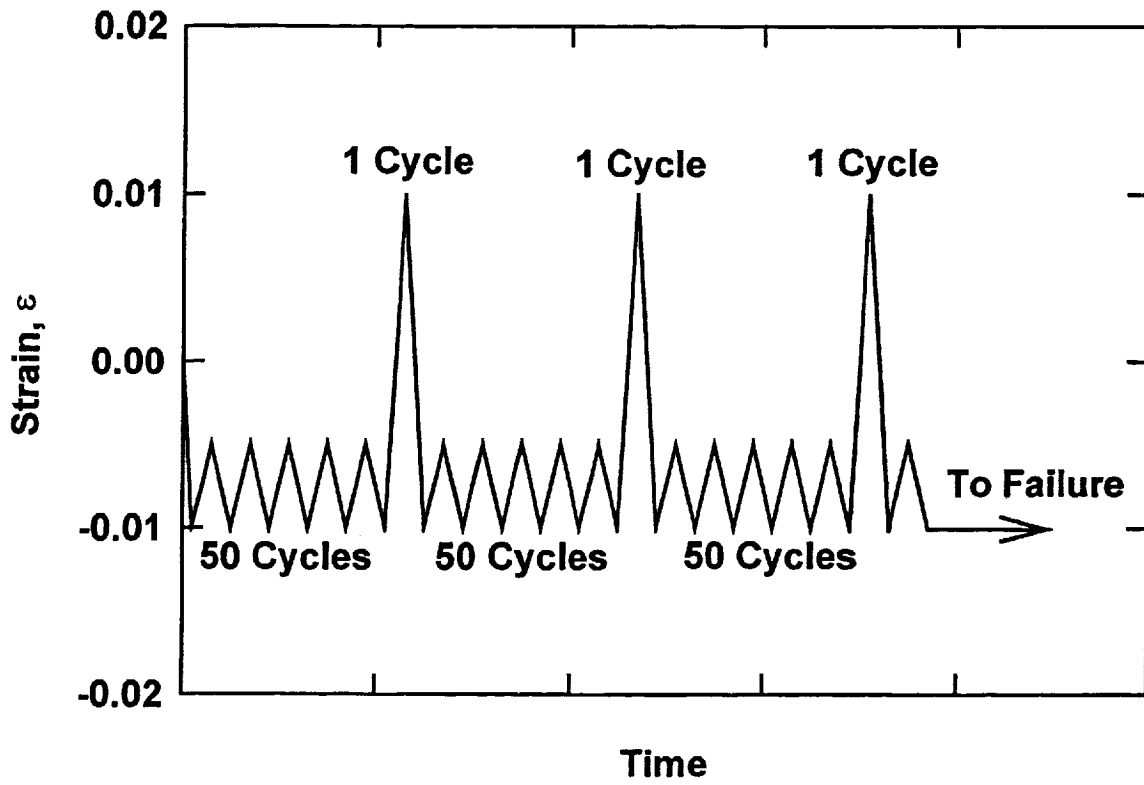
Fig. 4 -- Smith-Watson-Topper Fatigue Life Relation for Strain-Controlled Fatigue Data

($R_\epsilon = -\infty, -1, \text{ and } 0$) of Haynes 188 at 760°C



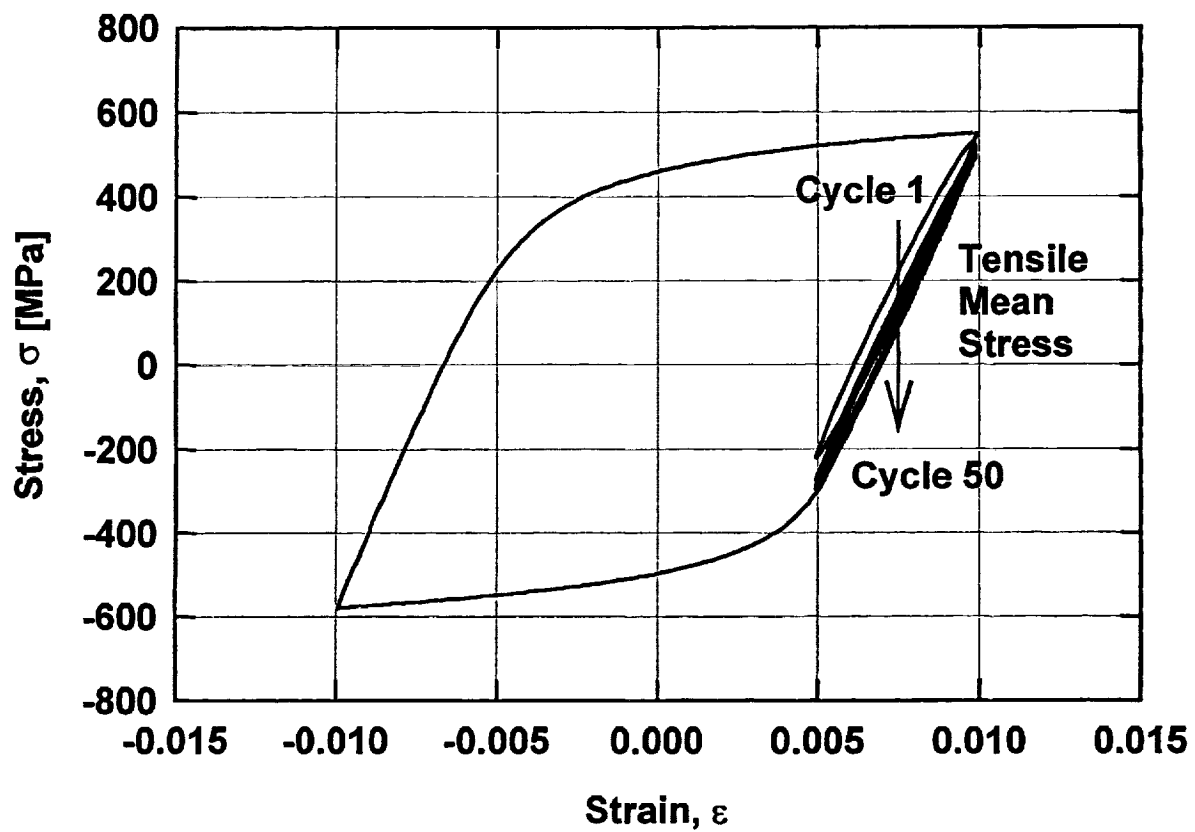
a) Block Loading, B1

Fig. 5 -- Schematics of Block Loading Patterns in Cumulative Fatigue Tests



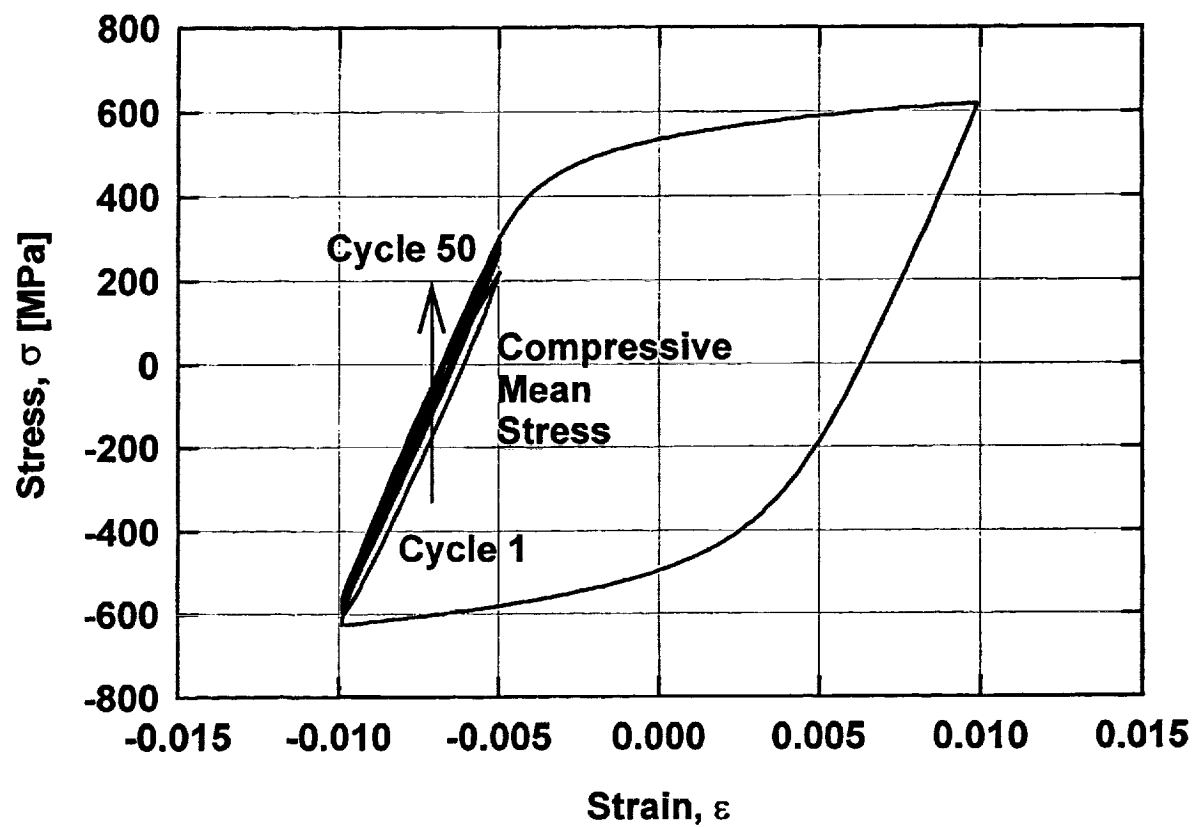
b) Block Loading, B2

Fig. 5 -- Schematics of Block Loading Patterns in Cumulative Fatigue Tests



a) Block Loading, B1

Fig. 6 -- Hysteresis Loops in Cumulative Fatigue Tests



b) Block Loading, B2

Fig. 6 -- Hysteresis Loops in Cumulative Fatigue Tests

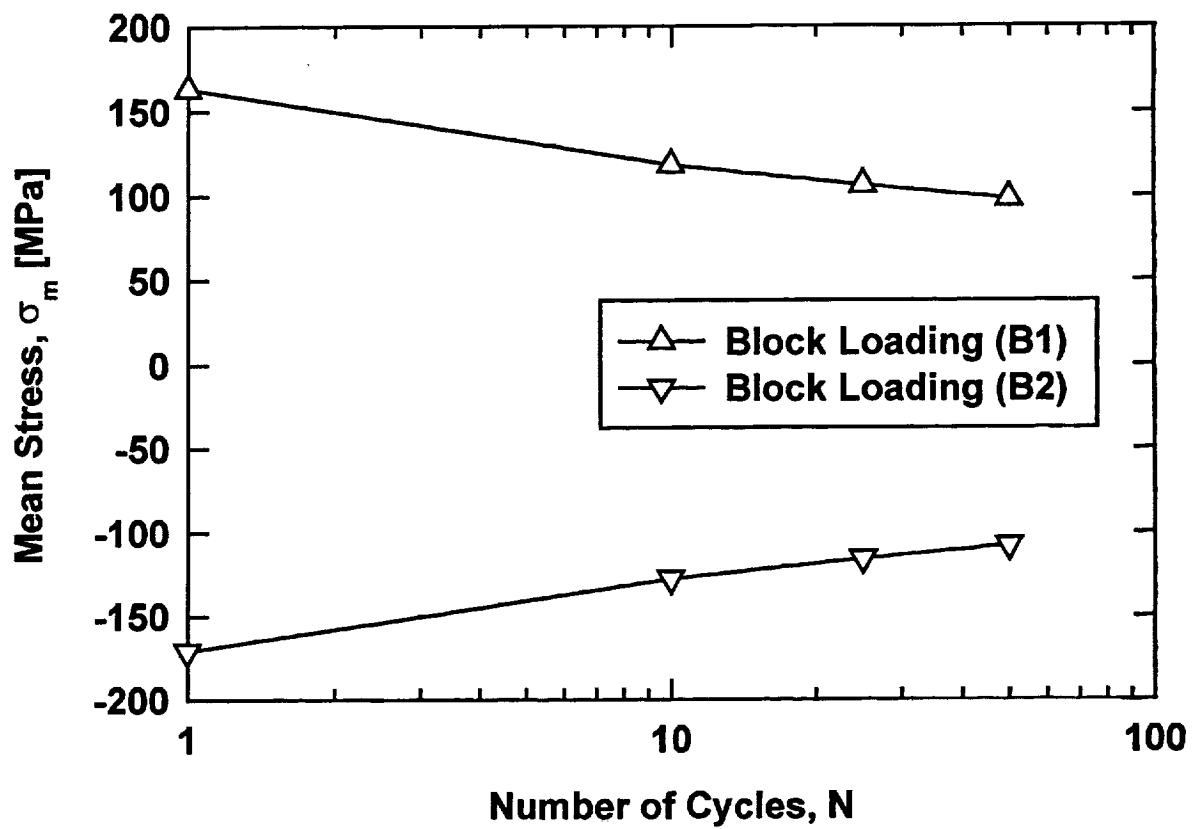


Fig. 7 -- Evolution of Mean Stresses in Cumulative Fatigue Tests

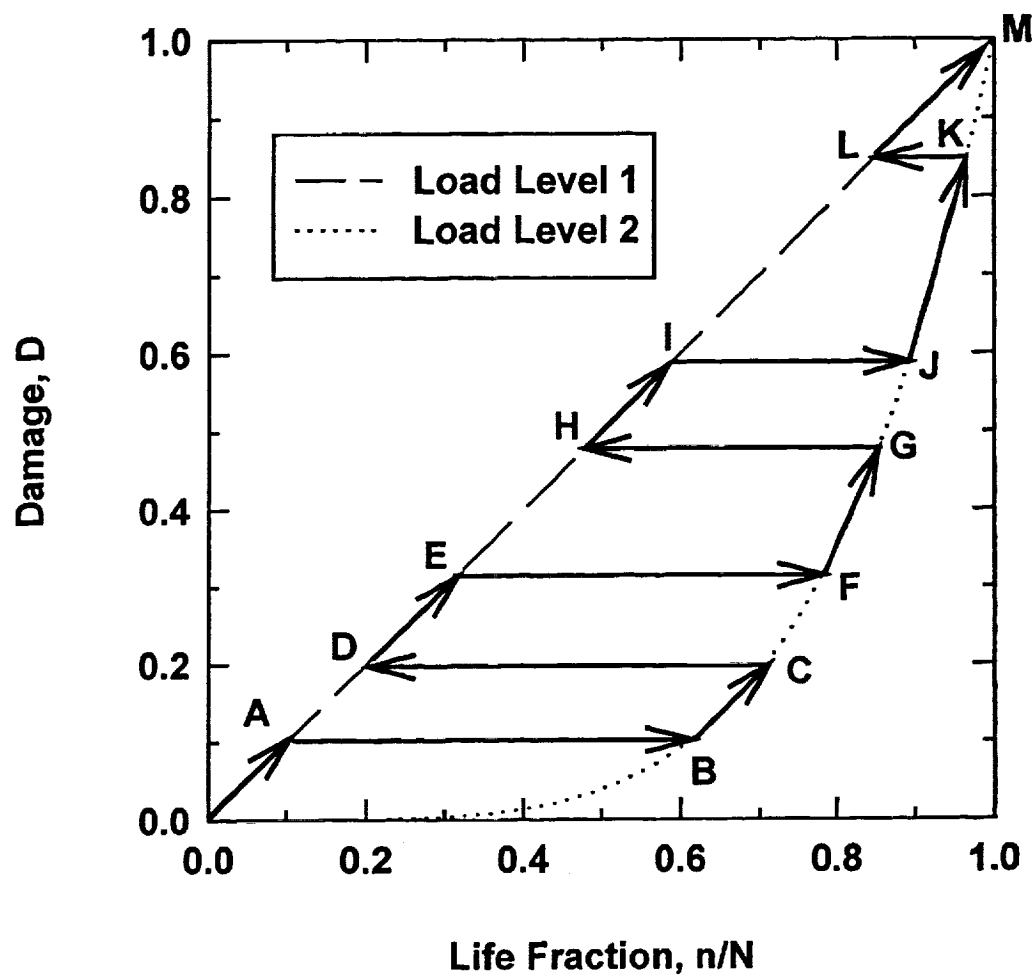
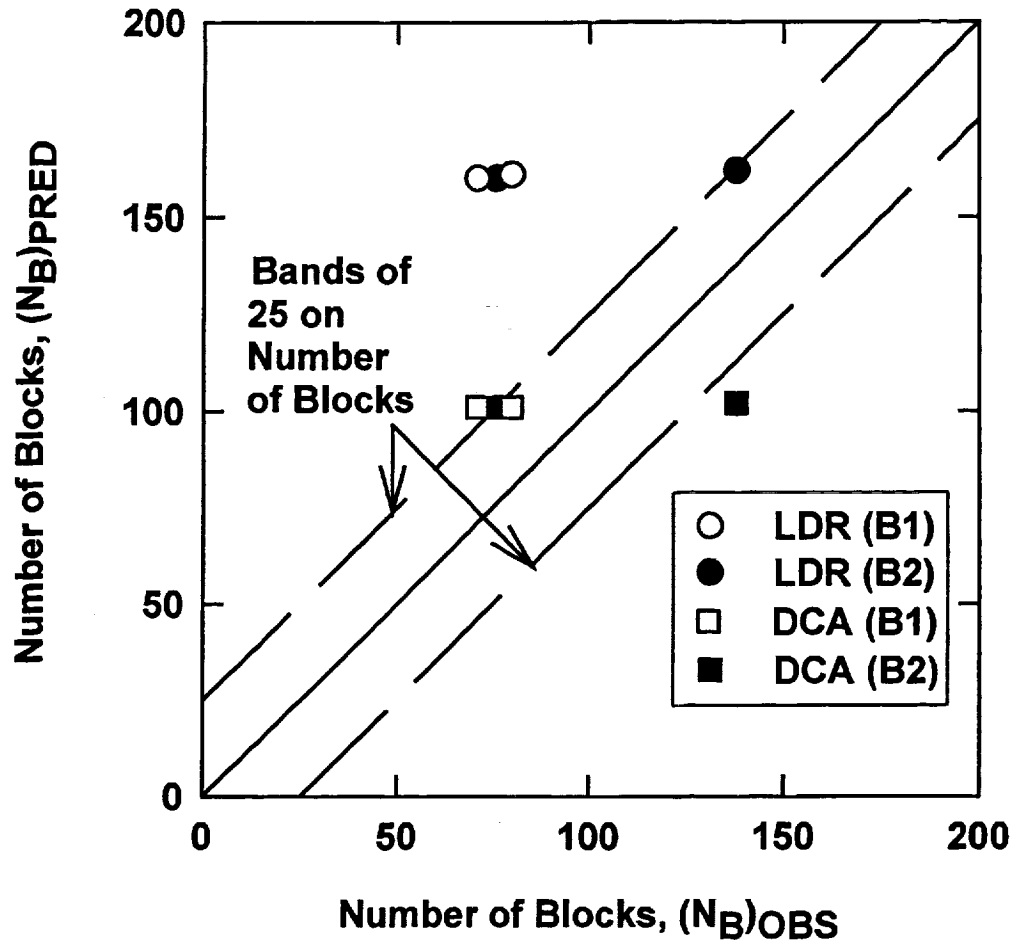
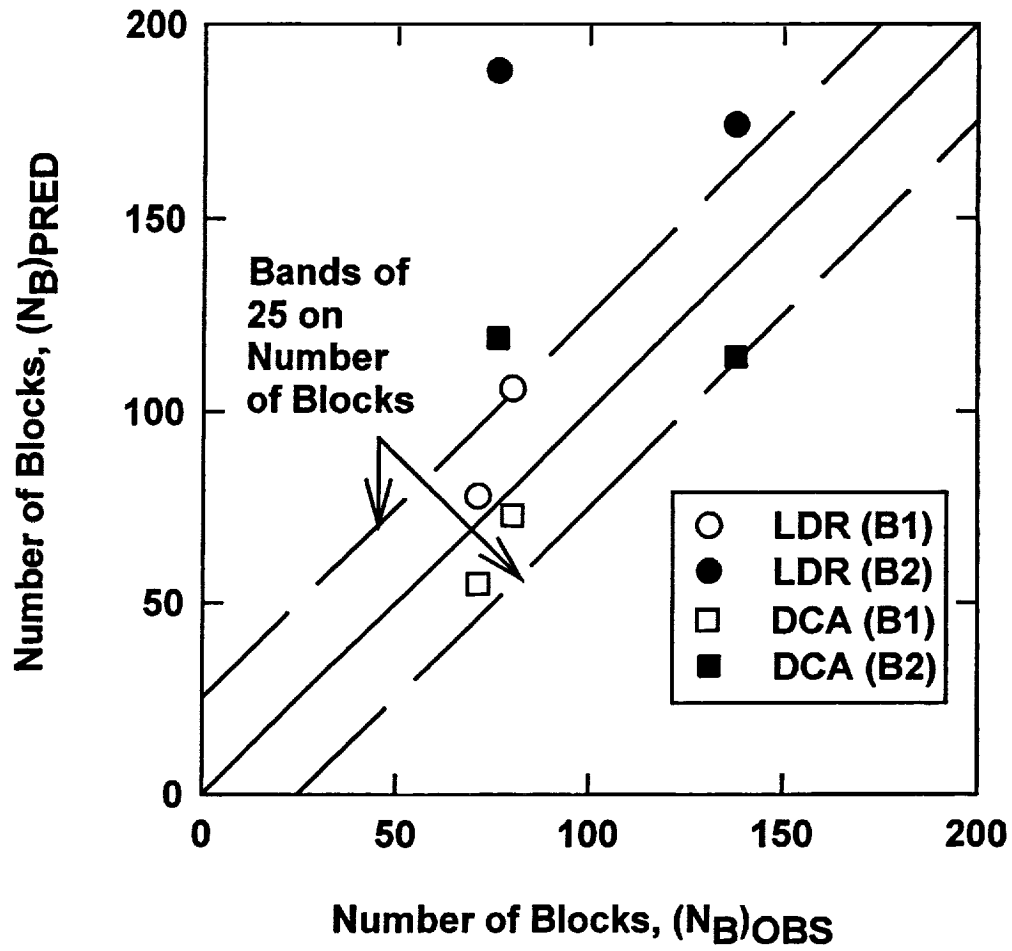


Fig. 8 -- Schematic of Damage Estimation in Two Load-Level Multi-Block Fatigue Tests
with Nonlinear Damage Curve Approach



a) Without Mean Stress Consideration

Fig. 9 -- Life Prediction of Cumulative Fatigue Tests: Haynes 188 at 760° C



b) With Mean Stress Consideration

Fig. 9 -- Life Prediction of Cumulative Fatigue Tests: Haynes 188 at 760° C